# Journal of Applied Sciences

ISSN 1812-5654

science alert

ANSInet
an open access publisher
http://ansinet.com

Journal of Applied Sciences 7 (19): 2710-2724, 2007
ISSN 1812-5654


# A Computational Fluid Dynamics Study of Cold-flow Analysis for Mixture Preparation In a Motored Four-stroke Direct Injection Engine

Wendy Hardyono Kurniawan, Shahrir Abdullah and Azhari Shamsudeen
Department of Mechanical and Materials Engineering, National University of Malaysia,
UKM Bangi 43600, Malaysia

**Abstract:** In this study, the Computational Fluid Dynamics (CFD) simulation to investigate the effect of piston crown to the fluid flow field inside the combustion chamber of a four-stroke direct injection automotive engine under the motoring condition is presented. The analysis is focussed on the study of the effect of the piston shape to the fluid flow characteristics. The fluid flow dynamics plays an important role for air-fuel mixture preparation to obtain the better engine combustion, performance and efficiency in the appearance of swirl and tumble flows. These two parameters represents the fluid flow behaviours occurred inside combustion chamber which influences the air streams to the cylinder during intake stroke and enhances greatly the mixing of air and fuel to give a better mixing during compression stroke. The numerical calculations were performed in a single cylinder of 1.6 L of a 4-stroke direct injection engine running at wide open throttle condition by using the CFD code. Two different piston bowls for considered engine speeds of 2000 rpm were considered to be compared to evaluate swirl and tumble flows produced during intake and compression stroke. The results obtained from the numerical analysis can be employed to examine the homogeneity of air-fuel mixture structure for better combustion process and engine performance.

**Key words:** Computational fluid dynamics, piston crown, swirl, tumble, fluid flow, air-fuel mixture

## INTRODUCTION

The in-cylinder flows of Internal Combustion Engine (ICE) have drawn much attention to the automotive researchers and scientist in the present times. It is due to the fact that the flow structure generated by intake flows is related closely to the design and performance of the ICEs. The production of high turbulence intensity is one of the most important factors for stabilizing the ignition process and fast propagation of flame, especially in the case of lean-burn combustion. In general, two types of vortices are utilized in order to generate and preserve the turbulence flows efficiently. These vortices are usually know as swirl and tumble flows, which are organized rotations in the horizontal and vertical plane of the engine cylinder, respectively. They contribute to the improvement of engine performance by accelerating mixing of fuel and induced air (Heywood, 1988). Hence, it is indispensable for the development of an ICE with high compression ratio to realize high turbulence intensity and lean burn combustion.

Quite a few experimental works in visualising in-cylinder flows have been conducted to measure velocity fields by using the hot wire anemometry or lased Doppler velocimetry (Stone, 1992). However, it is a really hard task to perform it because the measurements of in-cylinder flows in the reciprocating engine are characterized by highly complex three-dimensionality, turbulence and unsteadiness. A numerical approach could thus be an alternative because of the capability of CFD which has been developed for in-cylinder flow predictions in recent 20 years. Gosman (1984) work can be regarded as a pioneering one which applied CFD simulation to investigate in-cylinder flows and since then tremendous improvements have been achieved in computational techniques in this field of study. The CFD code of KIVA and STAR-CD are most frequently employed as a commercial package programs for in-cylinder analysis in the reciprocating engine in present days. This computer codes are utilised to solve the Navier-Stokes equations to produce detailed descriptions of the mean velocity and the turbulence velocity fields. While applying to the ICE case, the CFD models should cover the specific problems related the turbulent flow, high Reynolds number, compressible flow and the complex geometry model. Consequently, the computational times are usually costly and require huge computer memory and even High Performance Computing (HPC) facilities to reduce the work.

**Corresponding Author:** Wendy Hardyono Kurniawan, Department of Mechanical and Materials Engineering, National University of Malaysia, UKM Bangi 43600, Malaysia

Based on the literature studied, several researchers have conducted the research on the geometry of a combustion chamber to determine fluid flow using numerical methods. In the following, the previous study of the fluid flow during intake and compression stroke in ICEs will be highlighted according to its year of research done. Mao *et al.* (1994) had calculated the intake and compression strokes for an axisymmetric case using a finite element method. Chen *et al.* (1998) performed calculations of the full intake and compression processes and Dillies *et al.* (1997) also presented similar calculations of a Diesel engine with one intake valve for one combustion chamber. The simulation of the detailed in-cylinder air motion during intake and compression stroke to examine the interaction of air motion with high-pressure fuel spray injected directly into the cylinder also has been accomplished by Kim *et al.* (1999). Celik *et al.* (2001) made a review of computations based on large eddy simulation (LES) and concluded that this method has great potential in this kind of application; however its computational cost is still too high for engine design. In addition, Hyun *et al.* (2002) also has performed the numerical simulation by employing the CFD code of KIVA-3 whereby the shape of combustion chamber, swirl intensity and injection timing are modified and the effect of mixture formation is investigated. Sukegawa *et al.* (2003) and Wu and Perng. (2004) have performed in-cylinder flow analysis, but the shapes of its piston attached to the engine cylinder were relatively simple compared to the practical piston crown in any ICE. Lastly, Payri *et al.* (2004) who have carried out the CFD modelling of the in-cylinder flow in direct-injection Diesel engines for intake and compression stroke with different chambers. Among the engine researchers, many of them have not investigated yet the difference of piston shape to the distribution of in-cylinder air flow analysis, except the work done by Wu and Perng. (2004) with their simple piston head and Payri *et al.* (2004) with their real piston head. Therefore, a research study by mean of numerical approach by using the CFD code for in-cylinder air flow analysis and simulation with different piston shapes in an automotive four-stroke engine with direct injection system need to be carried out.

In this study, the CFD code of STAR-CD with the capability of moving mesh and boundary algorithms, including the valves and piston movement capability was employed in this study to investigate the effect of the piston crown shape to the fluid flow field. Other than that, the homogeneity of air structure for fuel mixing preparation that occurred inside engine cylinder was also assessed to determine the better piston crown. The motivation behind this study is that the fluid flow with different combustion chamber has an influence in air-fuel mixing preparation and generation of turbulence as well as exerts great impact on engine performance. Two different combustion chambers with realistic geometry utilised for a 4-stroke automotive engine with direct injection system will be considered in detail for in-cylinder flow calculations during intake and compression stroke. In this work, no simplifications of the geometry model and intake calculations involve intake port and moving valves was constructed so that the flow field could be analysed completely. The numerical calculation is performed to obtain the optimum parameters mentioned above for such engine, which influences to accomplish the better air and fuel mixing for the rapid combustion process. In order to study the effect of the combustion chamber shape to the fluid flow field, two characteristics of large scale mixing were analysed in-depth to identify the behaviour of swirl and tumble flow along degree of crank angle.

The numerical computation was executed using the transient analysis of intake and compression stroke for two piston crown, which equipped with its boundary conditions. The engine speed considered in this work is 2000 rpm with the fixed valve timing and lift. The two parameters for the fluid flow characteristics acquired from the simulation will be taken into account to verify the homogeneity of air structure for mixture preparation so that the better air-fuel mixture and combustion process can be achieved. In particular, the differences observed for the two different piston bowl shapes in the parameters configuration of fluid flow characteristics during intake and compression stroke are discussed and some conclusions can be drawn out. From the observation, the optimum shape of piston crown can be determined and chosen for the improvement of combustion processes in order to obtain the better engine performance and emissions. It is expected that the present study will provide an insight of the influence of the piston bowl on the characteristics of air structure pattern for a direct injection engine. In addition, the present CFD study can be used as a research tool to observe the complexity of fluid dynamics inside engine cylinder. This research can be carried out to provide the alternative method instead of the experimental equipment of Particle Image Velocimetry (PIV) or Laser Doppler Anemometry (LDA).

## CFD MODELLING OF ICE PROCESS

The CFD simulations of this study were performed for intake and compression strokes by using the moving mesh-boundary algorithm. Every contained event represents the different mesh and boundary geometries for every different crank angle in each step of engine cycle. Hence, in order to perform the proper CFD

simulations for an internal combustion process, the analysis and calculation should be carried out by using the unsteady (transient) calculation, moving meshes and boundaries, high compressible Reynolds number, high fluid dynamics characteristics (turbulence intensity), momentum, heat and mass transfer and complex geometries model and chemical-thermal dependent as well.

The equations employed to describe mass, momentum, energy and k-ε turbulence model in the vector notation without source terms from spray and chemical reactions due to under motoring condition are expressed as follows:

$$\frac{\partial \rho}{\partial t}+\nabla\cdot\left(\rho\vec{u}\right)=0 \quad (1)$$

$$\frac{\partial \rho}{\partial t}\left(\rho\vec{u}\right)+\nabla\cdot\left(\rho\vec{u}\vec{u}\right)=\nabla P-\nabla\left(\frac{2}{3}\rho k\right)+\nabla\cdot\overleftrightarrow{\sigma}+\rho g \quad (2)$$

$$\frac{\partial \rho}{\partial t}(\rho I)+\nabla\cdot\left(\rho I\vec{u}\right)=-P\left(\nabla\cdot\vec{u}\right)-\nabla\left(\frac{2}{3}\rho k\right)+\nabla\cdot\vec{J}+\rho\varepsilon \quad (3)$$

$$\frac{\partial}{\partial t}(\rho k)+\nabla\cdot\left(\rho\vec{u}k\right)=-\frac{2}{3}\rho k\nabla\cdot\vec{u}+\overleftrightarrow{\sigma}\cdot\nabla\vec{u}+\nabla\left[\left(\frac{\mu_t}{Pr_k}\right)\nabla k\right]-\rho\varepsilon \quad (4)$$

$$\frac{\partial}{\partial t}(\rho\varepsilon)+\nabla\cdot\left(\rho\vec{u}\varepsilon\right)=-\left(\frac{2}{3}c_{z1}-c_{z3}\right)\rho\varepsilon\nabla\cdot\vec{u}+\nabla\cdot\left[\left(\frac{\mu_t}{Pr_\varepsilon}\right)\nabla\varepsilon\right]+\frac{\varepsilon}{k}\left[c_{z1}\overleftrightarrow{\sigma}:\nabla\overleftrightarrow{u}-c_{z2}\rho\varepsilon\right] \quad (5)$$

where, $\rho$ is the density; $\vec{u}$ the velocity vector; P the pressure; $\overleftrightarrow{\sigma}$ the turbulent viscous stress tensor; I the specific internal energy and $\vec{j}$ the heat flux vector including turbulent heat conduction and enthalpy diffusion effects.

## ENGINE GEOMETRY AND OPERATING CONDITION

The engine model studied is a typical single-cylinder of a CNG-DI engine with two intake and exhaust valves as shown in Fig. 1 equipped with two considered pistons shapes (Fig. 2). As mentioned, two piston crowns were considered to investigate the behaviour of swirl and tumble flows occurred inside cylinder in order to obtain the suitable piston shape for the combustion process of such engine. These two shapes are representative of the real engine geometry model that usually operated to obtain the higher compression ratio as well as the optimum combustion process in a CNG-DI engine. Piston A has a bowl at the centre of its crown piston while piston B has the deeper bowl volume than piston A and is not located in the centre of its crown.

Fig. 1: A schematic view of typical engine model with piston crown A

Piston A Piston B

Fig. 2: Geometry of the combustion chamber

Table 1: Specification of the engine model for computational condition

| Engine parameters | Value | Unit |
|---|---|---|
| Number of cylinders | 4 | - |
| Type | Inline | - |
| Displacement volume | 1596 | $cm^3$ |
| Bore | 78 | mm |
| Stroke | 84 | mm |
| Connecting rod length | 131 | mm |
| Crank radius | 44 | mm |
| Compression ratio | 10 | - |
| Intake valve opening | 12 | bTDC |
| Intake valve closing | 48 | aBDC |
| Exhaust valve opening | 45 | bBDC |
| Exhaust valve closing | 10 | aTDC |
| Maximum intake valve lift | 8.1 | mm |
| Maximum exhaust valve lift | 7.5 | mm |
| Combustion chamber | Bowl piston | - |

The specifications and characteristics of operating condition from engine model studied that will be employed for the computational study and boundary condition of CFD analysis during intake and compression stroke summarised in Table 1.

## NUMERICAL METHODOLOGY

The CFD code of STAR-CD for finite volume method has been utilised to solve the discretized continuity and Navier-Stokes equations. This CFD code is commonly used for ICE and has the high capability of solving the transient, compressible, turbulent-reacting flows with sprays on the finite volume grids with moving boundaries and meshes. Fully hexahedral meshes of intake and exhaust ports and combustion chamber are utilised here due to the requirements of moving mesh. Piston and valve motion are carried out by cell activation and deactivation and supported by vertex motion routines. The code is competent of handling the complex geometry and enabling the computational domain to include intake and exhaust ports, valves, valve seats and the combustion chamber with moving piston.

The numerical methodology and computation of this ICE case is based on the pressure-correction method and the PISO (pressure implicit with splitting of operators) algorithm. The second upwind differencing scheme (MARS) as the spatial discretization is used for the momentum, energy and turbulence equations. The temporal discretization is the implicit method, with variable time step depending on the stage of the engine cycle. At the beginning and the end of intake stroke, when the valve lift is quite small, there are high local velocities in the discharge zone. Therefore, the time step must be small enough as 0.1 CAD per iteration) in order to accomplish the stability criterion (Versteeg and Malalasekera, 1995). During the middle phase of intake stroke and also during the compression stroke, before the piston reaches TDC, the time step is set up at the 0.25 CAD per iteration by reason of the highly computational cost since there are no high local velocities. In addition, the valve positions have been closed and the effect of air flow during compression stroke to the numerical stability of CFD calculation is not too highly influenced. Finally, near TDC, the time step must be reduced again to 0.1 CAD per iteration because of the effect to tumble and the small clearance between the piston and the cylinder head.

The running calculations started when intake valve opening and continued to the compression stroke without the fuel injection. These both variables are calculated as homogeneous in the whole domain. The valve overlap period is also taken into account when the residual gases come out from the exhaust port. The initial values for pressure and temperature for engine operating speed of 2000 rpm were obtained from the experimental work and test from a single cylinder research engine test bed. The initial turbulence intensity was set at 3% of the mean flow, which is quite sufficient for fully turbulent fluid flow, whereas the integral length scale was specified proportional at 0.4% based on the Prandtl's work as a result of the distance to the nearest solid wall (Launder and Spalding, 1974). Constant pressure boundary conditions were carried out at both intake and exhaust ports so that the dynamics effects were neglected. The walls of intake and exhaust ports and the lateral walls of the valves were considered as the adiabatic condition. The constant temperature boundary conditions were allocated independently for the cylinder head, the cylinder wall and the piston crown that outline the walls of the combustion chamber. The temperature on each of these walls will be calculated numerically in the form of iteration for every time step automatically.

## GRID GENERATION

A grid generation program has been exploited to generate the grid to create the hexahedral cells for the engine model. The computational domain for the CFD calculation covers intake ports and valves, the cylinder head and the piston bowl as shown in Fig. 3. The number of cells varies from 90,000 cells in Top Dead Centre (TDC) position and around 180,000-200,000 cells in Bottom Dead Centre (BDC) position, where about the half of the cells used to generate the mesh at the cylinder head and piston bowl in the case of considering the grid sensitivity and reasonable computer run time. The fine grid structure is necessary for mesh snapping during the valve movement. The hexahedral cells have been adopted for the mesh generation because they provide a better accuracy and stability compared to the tetrahedral cells. The much important motivation about the use of hexahedral cells is the requirements of moving meshes and boundaries to accomplish the CFD calculation.

Because of complexity of the engine model, the computational mesh is divided into four areas with different topologies, where each area has been meshed separately as shown in Fig. 4. This approach is used to obtain a good quality grid (mesh) and to reduce the meshing time significantly. The connectivity of the various sub-domains is ensured by means of arbitrary interfaces that connect every faces of the zones. Both intake ports meshes have been created using a similar topology, where the cell are oriented in the flow direction and joined with a cylindrical structured mesh in the zone upstream of the valves. The grid above the valves both intake and exhaust has been constructed by the revolution of a structure mesh section. During the compression stroke, when intake valves are closed, the

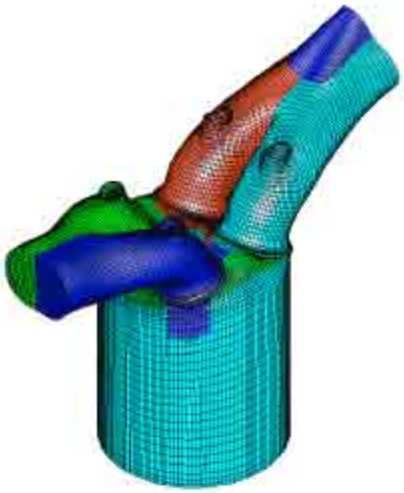

Fig. 3: The computational domain of the engine model

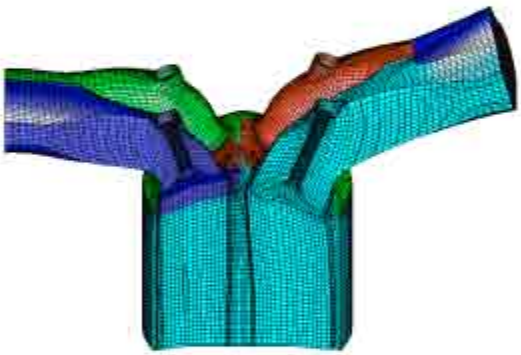

Fig. 4: The clipped section view of the computational domain

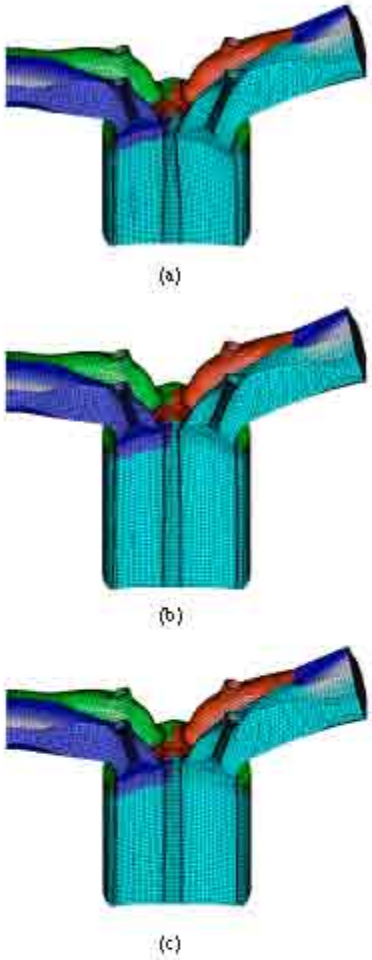


Fig. 5: The moving mesh intake stroke (a), bottom dead centre (b) and compression stroke (c)

sub-domains of intake ports are already disconnected from the calculation to reduce the computational time and cost as well.

As mentioned above, the simulation required a moving mesh and boundary algorithm embedded into the STAR-CD programme. The moving mesh and boundary algorithm for this engine model has been developed inside STAR-CD by declaring the events for each time step we define and then activating the grid in order to move the mesh. The concept of moving mesh is that the cell is squeezed to zero volume over one time step, with all its contents (pressure, temperature, mass, momentum, enthalpy, etc.) being expelled into the neighbouring cells. Hence, conservation is satisfied exactly even with removal of any cell layer. On the other hand, when the cell layers are added, they grow from zero size to their full volume, absorbing the conserved variables through their faces (CD Adapco, 2004). Some examples of moving meshes and boundaries developed for the CFD simulation model are given in Fig. 5, which are intake stroke, the position of piston at BDC and the compression stroke. As the total number of computational cell is around 180,000-200,000 cells, the typical CPU time taken for the simulation of complete intake and compression stroke with the fluctuate time steps is around 10 hours on a 4 CPU-SGI Origin 300 with 56 MB dynamic memory used during the running analysis.

A grid dependency test for the engine computational mesh has been performed for the purpose of checking the finer mesh configuration employed in this study. The refined mesh has the more quarter number of cells (Fig. 6b) as the second case than the current mesh

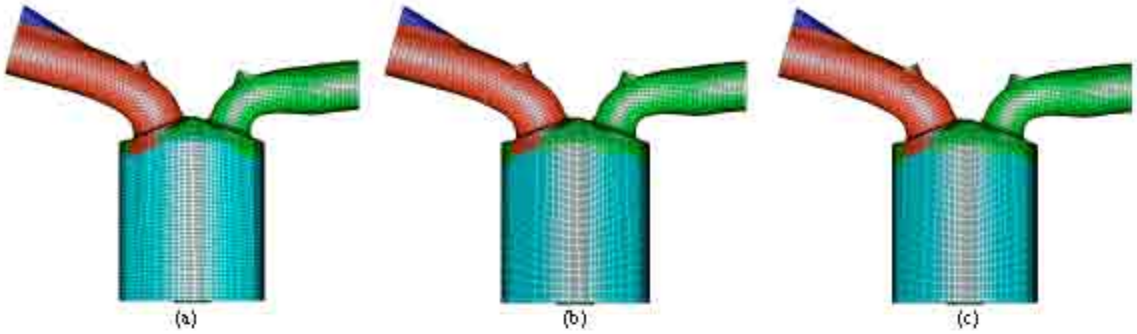


Fig. 6: A grid dependency test of engine computational configuration

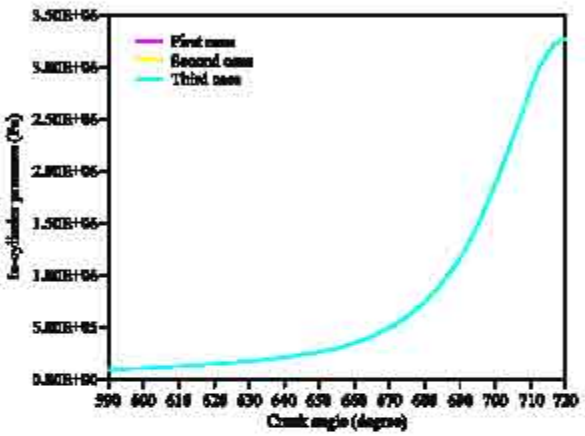


Fig. 7: In-cylinder pressure for a grid dependency test

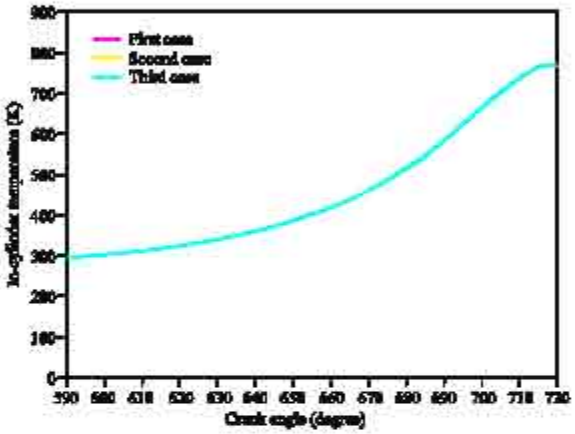


Fig. 8: In-cylinder temperature for a grid dependency test

configuration (Fig. 6a) as the first case. On the other hand, the third case is the mesh configuration with half finer mesh (Fig. 6c) than the first case. The performed grid independence study has proved that the quarter and half finer mesh does not influence to the solved numerical parameters, such as cylinder pressure and temperature as shown in Fig. 7 and 8, respectively. From the point of view of the comparison parameters presented here, it is also representative of the results in other parameters of the combustion chamber, such as swirl ratio, tumble ratio and turbulence velocity field. As can be seen in Fig. 7 and 8, there are no significant differences between the CFD solutions obtained between the three compression calculations. However, the CPU costs are nearly tripled in the case of the refined computational mesh and it does not give the advantages to the CFD calculation. Therefore, it can be concluded that the current normal mesh can be used to obtain the numerical stability and accuracy for the present in-cylinder flow analysis.

## RESULTS AND DISCUSSION

The detailed numerical study to investigate the effect of the piston crown shape to the fluid flow field characteristics for a 4-stroke direct injection engine under motoring condition has been carried out. The results presented are discussed for fluid flow field characteristics, together with its discussions for the two different piston crowns. In addition, the graphs of global variations for each parameter are plotted according to degree of crank angle.

Here, the velocity vector field as the large-scale mixing during intake and compression stroke in the cylinder for two piston crown will be analysed and investigated. To analyse in-cylinder air motion inside the cylinder, swirl and tumble ratios for both on the sideways and normal directions are calculated at each time step or every crank angle degrees of engine cycle to identify the behaviour of fluid flow field characteristics among two different piston shapes.

As mentioned previously, swirl and tumble flows are always generated during intake and compression stroke of ICE due to the high turbulence in the cylinder. Swirl refers to a rotational flow within the cylinder about its axis and is used to promote rapid combustion. And tumble is a rotational motion about a circumferential axis near the edge of the clearance volume in the piston crown or in the cylinder head, which is caused by squishing of the in-

cylinder volume as piston reaches near TDC. Both swirl and tumble flows are commonly characterized by a dimensionless parameter employed to quantify rotational and angular motion inside the cylinder, which are known as swirl and tumble ratios, respectively. These values are calculated by the effective angular speed of in-cylinder air motion divided by the engine speed. The effective angular speed is the ratio of the angular momentum to the angular inertia of moment. The mass centre of the charged in-cylinder air is considered as an origin for the calculation.

In order to facilitate the comparison of the results under different piston shapes, the three variables (swirl, sideways tumble and normal tumble ratio) plotted in this study are presented in the non-dimensional form by applying the equations as follows:

$$SR = \frac{60H_z}{2pI_z\omega} \quad (6)$$

$$TR_x = \frac{60H_x}{2pI_x\omega} \quad (7)$$

$$TR_y = \frac{60H_y}{2pI_y\omega} \quad (8)$$

where, $H_x$, $H_y$ and $H_z$ is the angular momentum of the in-cylinder gas about the x axis, y axis and z axis, respectively. $I_x$, $I_y$ and $I_z$ is the moment of inertia about the x axis, y axis and z axis, respectively. In addition, $\omega$ is the crankshaft rotation or engine speed in the unit of rotation/minute. A schematic view of reference axes for the analysis and calculation is presented in Fig. 9. The origin of the coordinate systems shown in the figure is only for a reference to illustrate swirl and tumble directions and magnitudes.

The in-cylinder air motion before fuel injection process is such important to certify a proper air-fuel mixture, which finally affects on the complete combustion in the engine cylinder. In the following some details of in-cylinder air motion without fuel injection during intake and compression stroke for the engine speed of 2000 rpm are figured out to describe the velocity vector in the forms of swirl and tumble flows.

Figure 10 shows the velocity fields during intake stroke (100° after TDC) for two combustion chambers on the XY cutting plane (at Z = 10 mm of cylinder head axis) as shown in the top figure, the XZ cutting plane (at Y = 7 mm) as shown in the middle figure and the YZ cutting plane as shown in the bottom figure. It can be seen that there are strong annular jet flows for two combustion chambers in the area near the valve curtains because the flow and velocity field in this degree of crank

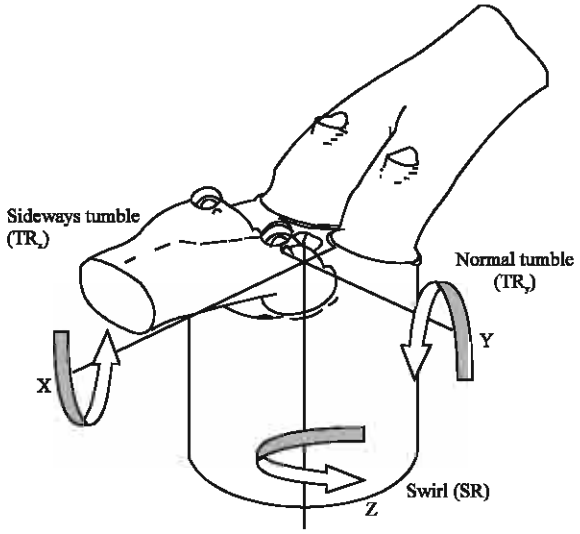


Fig. 9: Schematic view for the definition of swirl and tumble axes and directions (SR: swirl ratio, $TR_x$: sideways tumble ratio, $TR_y$: normal tumble ratio)

angle reaches to the maximum value where intake valves almost open at the maximum lift distance. And this strong annular jet flows make a clockwise swirl on the one intake valve and a counter-clockwise on another intake valve as shown clearly for each piston crown shape. At this stage, the piston speed is nearly constant and intake valves are almost fully open (maximum lift). The toroidal vortex that developed in the early part of intake stroke has already disappeared. Nevertheless, a new clockwise vortex can be seen in the centre of the engine cylinder, especially under intake valves as a result of the jet motion towards the central part of the cylinder, which does not collide directly with the cylinder walls. This annular jet flows that impinges on the wall is deflected axially towards the piston with centre bowl and produces an elongated vortex along the wall. In addition, the top figure confirms that there are several vortices exist with no predominant pattern and there is symmetry flow field due to a vertical plane situated between the two intake valves.

During the later phase of the compression stroke, the axial upwards field encourages a gradual increase of the swirl velocity in the top part of the piston crown as shown in Fig. 11 for two piston crowns. It also can be pointed out that when the piston at the position of 30° before TDC, the axial velocity vector of air in the engine cylinder is practically complete to be mixed with the fuel in many areas or zones. During the compression stroke, the turbulence generated by the annular jet flows during the previous intake stroke decay quite quickly and remains seem to be distributed homogeneously along the engine

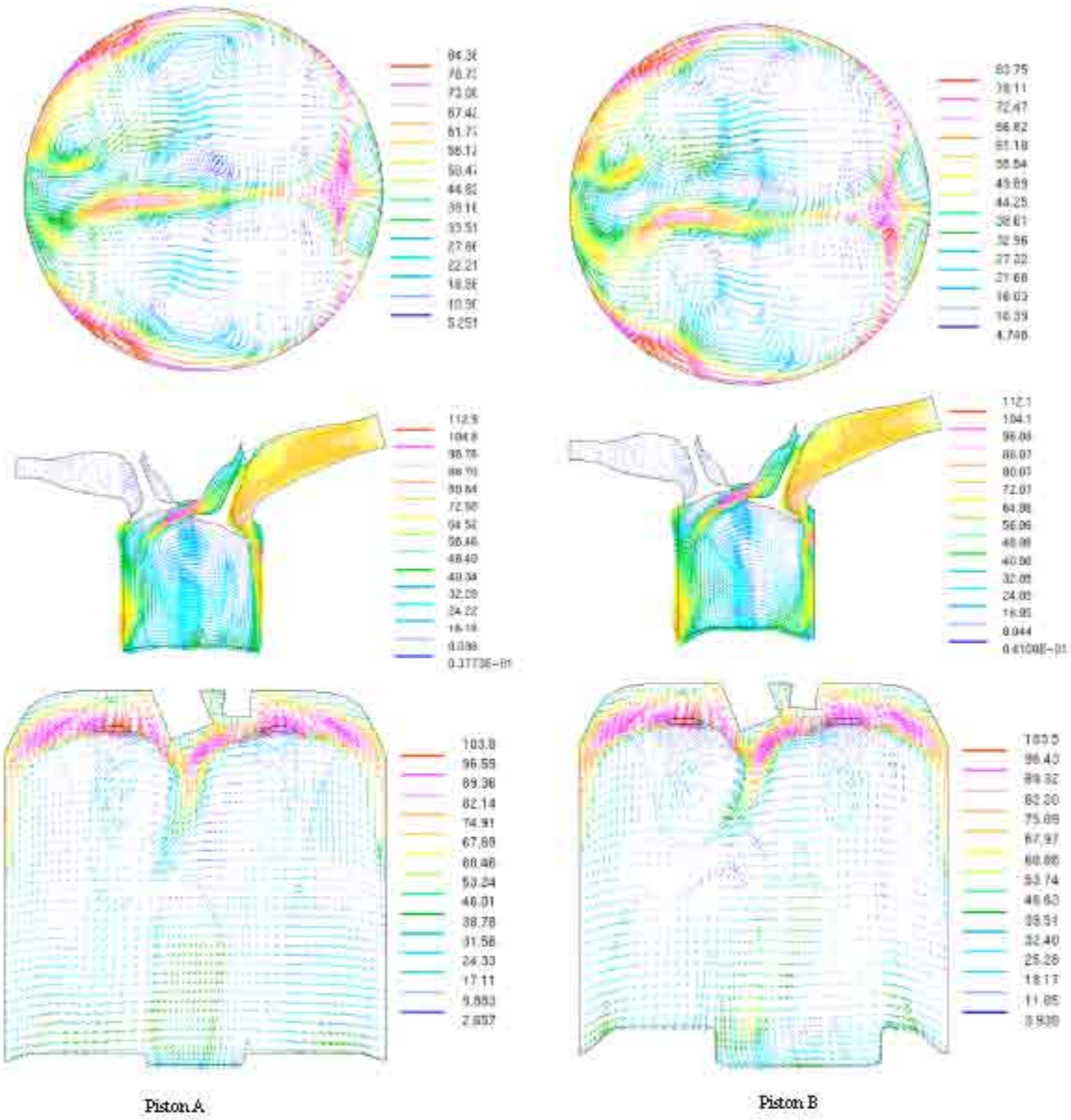


Fig. 10: Velocity vector field during intake stroke (100° after TDC) on the XY plane (top), XZ plane (medium) and YZ plane (bottom)

cylinder. The combustion chamber shape of an ICE is basically does not alter the global in-cylinder air motion but it is affect to the velocity field close to the piston top surface (near cylinder head) during the later phase of compression stroke where the fuel injection start to begin and the spark plug is ready to burn the air-fuel mixture to start off the combustion process. One important thing to be noticed from the present in-cylinder analysis of the engine is that the composition of air mixture within cylinder is homogeneous enough before the fuel is injected directly into the piston bowl and then ignited by spark plug to start the combustion process.

The global variations of swirl ratio for the two pistons are calculated and displayed in Fig. 12. For the purpose of computing swirl ratio, the reference values for x and y are taken at the cylinder axis where x = 0 and y = 0. As can be seen from the graph, the swirl in the cylinder is generated early during the intake stroke. The maximum is achieved

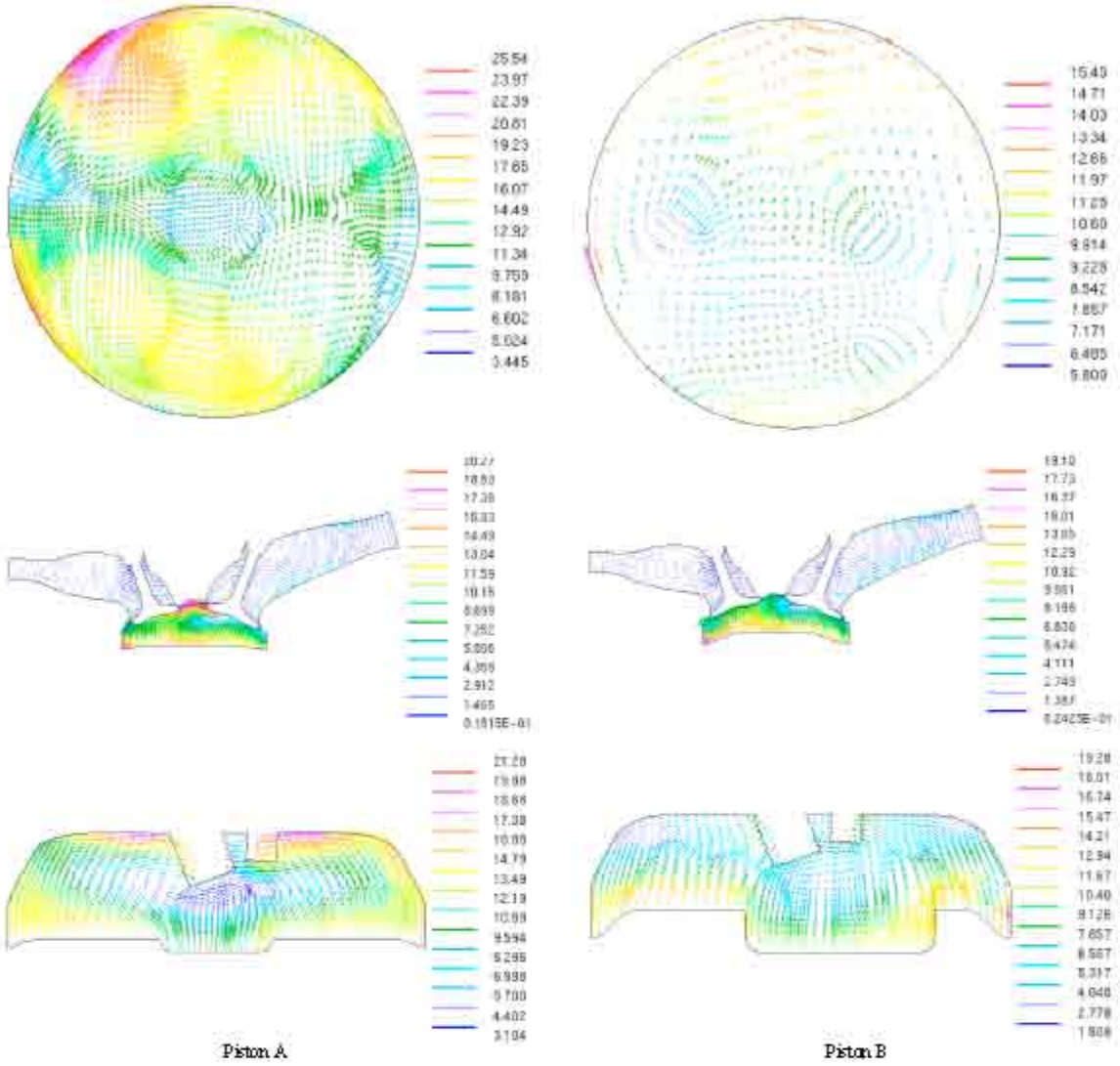


Fig. 11: Velocity vector field during compression stroke (30° before TDC) on the XY plane (top), XZ plane (medium) and YZ plane (bottom)

near around 140° after TDC, where the piston reaches its maximum instantaneous speed and the valve opening is in its maximum distance. After that, the discharge velocity into the cylinder decreases and swirl will decline slowly during the rest of the intake stroke. In the first part of the compression stroke, the trend continues to decrease due to the friction at the cylinder wall. However, swirl is developed as the flow accelerates in preserving its angular momentum within the smaller diameter piston bowl when approaching TDC. During the compression stroke, swirl is necessary needed to interact with squish flow to generate a very complex flow field for the purpose of enhancing air-fuel mixture during fuel injection. In fact, piston A is able to generate higher swirl ratio than piston B with small range differences during intake and compression stroke. From the analysis, it can be verified that the capability of producing swirl ratio for two different combustion chambers at same engine speed is relatively different due to the friction within cylinder wall and its intake air flows influenced by combustion chamber head.

Subsequently, the behaviour and variation of tumble flow in the sideways direction inside engine cylinder can be seen in Fig. 13. Tumble about the *x*-axis becomes negative in the early of the intake stroke and reaches a minimum at around 60° after TDC. After this crank angle,

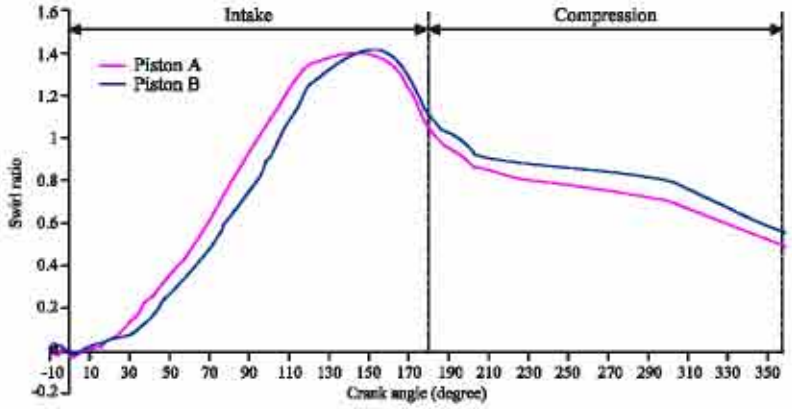


Fig. 12: Calculated swirl ratio versus crank angle

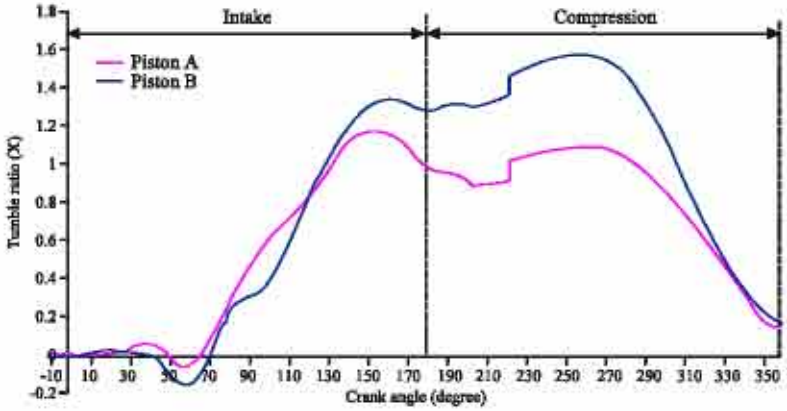


Fig.13: Calculated sideways tumble ratio versus crank angle

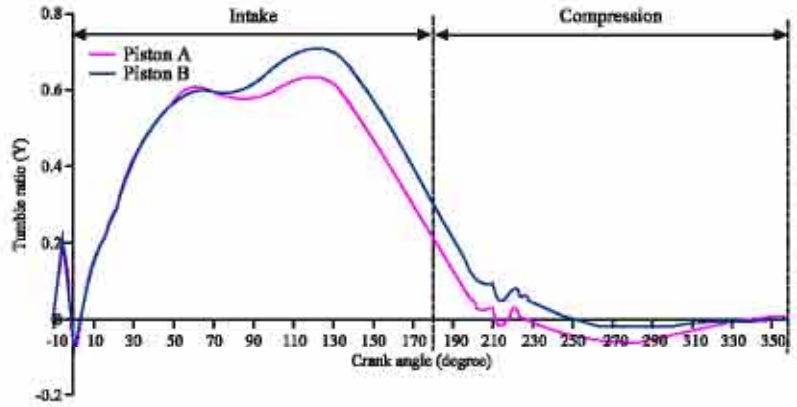


Fig. 14: Calculated normal tumble ratio versus crank angle

there is a quick change, which leads to a maximum positive tumble at around 150° after TDC. This difference condition can be attributed to the development of the two dominant vortices caused by the jet-bulk flow interaction. As the valve lift near to the closed position, the tumble ratio at the x-axis will be decreased gradually until the early part of the compression stroke before going up again during the middle of the compression stroke. After that, the sideways tumble ratio will decrease at the certain degree of crank angle near TDC. The extraordinary thing to be mentioned here is that the piston B produces the much lower magnitude of sideways tumble ratio along the

rest part of the compression stroke. This condition means that the piston B is not able to produce the homogeneity of air structure along cylinder, which needed to prepare the condition for fuel injection period.

The investigation of tumble ratio in the normal direction finally can be figured out in Fig. 14. The figures show the normal tumble ratio and its variation occurred inside engine cylinder. Tumble about the *y*-axis begins with a negative sense and changes its sign dramatically at the early part of intake stroke. This transient behaviour is characterized to the very complex nature of the early flow field. By 120° after TDC, a dominant tumbling motion has been developed and decreased incrementally as the valve lift closes until the early part of the compression stroke. And then, it will increase again slightly at the middle part of the compression stroke before diminishing again as piston approach TDC. From Fig. 14, it can be concluded that piston A can generate higher tumble ratio on the normal side (y-axis) during early intake stroke.

From the performed CFD study, the computational approach has showed that piston A has the capability of producing the higher swirl ratio and higher normal as well as sideways tumble ratios. This occurs due to the reason that the shape of piston plays an important role to the swirl and tumble ratio as the maximum intake valve lift occurred during intake stroke. This circumstance means that the shape of piston A plays an important role in producing the fluid dynamics parameters during intake and compression stroke as it has been determined from CFD analysis that piston A has the capability of producing better fluid flow field characteristics.

In addition to the expression of velocity field as swirl and tumble ratio, the turbulence field within combustion chamber can be depicted in the present research. It is presented in non-dimensional form by normalizing the value by the mean piston speed $V_p$. The turbulent velocity evolution in the two piston geometries considered was given in Fig. 15. In the CFD calculations, the fluctuating turbulent velocity is given by $(2k/3)^{0.5}$ according to the assumption of isotropic turbulence in the k-ε model for high Reynolds number. The turbulent velocity decays almost linearly as it approaches TDC and will start its downward motion during the expansion stroke. Since the bowl geometry is open for two piston crowns, the radial motion is weak and the squish effect small, which are located relatively far from the walls. It is also clear that the turbulence generation rate is faster than the turbulence dissipation rate. The highest turbulence velocity peaks appear during the maximum opening of intake valves due to the high velocity speed at the area of valve curtain. The magnitude of turbulence velocity will be increased a bit after BDC position and then continue to decrease until approaching TDC. The turbulence velocity of piston A is higher than that of piston B due to its smaller piston crown shape and it gives an advantage because the turbulence generation rate is high as the turbulence dissipation rate is small. The smaller piston bowl of piston A has an effect to the incoming air as it is more easily to suck the fresh air into the combustion chamber and results in higher velocities around the valve curtain area during the maximum intake valve opening. Therefore, the higher turbulence generation rate has been proved by the

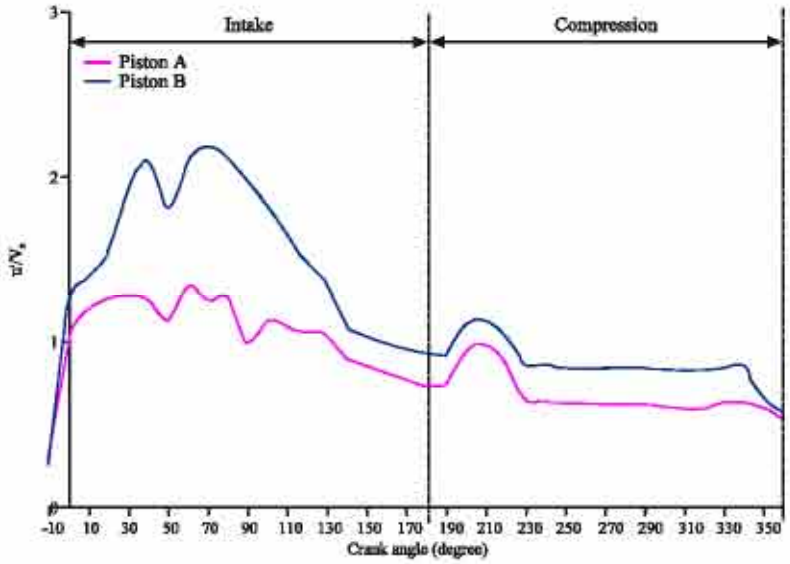


Fig. 15: Calculated turbulence velocity versus crank angle

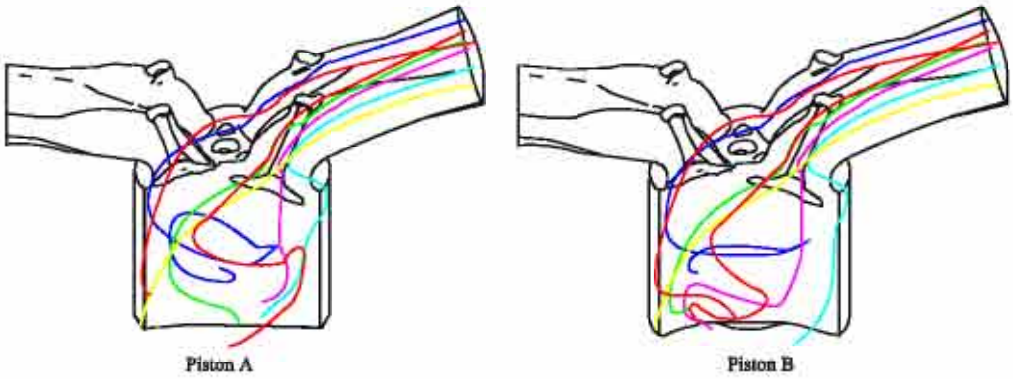


Fig. 16: The computed streamlines at 108° after TDC (intake stroke)

CFD calculation that it is produced by piston A. In conclusion, the turbulence model for high Reynolds number employed in this study is thus able to adequately capture these strong velocity fluctuations. In addition, it has been numerically verified that the isotropic turbulence assumption of the k-ε model is reasonably accurate for calculations of the in-cylinder flow, particularly in open combustion chambers, where there is strong interaction between swirl and squish and more generally in zones of the cylinder where the radial flow does dominate the flow pattern occurred.

Lastly, the other in-cylinder feature characteristic to examine the air flow inside cylinder and perceive the effect of combustion chamber shape is the unsymmetrical structure of the flow (Fig. 16). In this figure, the instantaneous streamlines at 108° after TDC, represented by continues lines, are shown. There are some streamlines presented to simulate the air-flow motion inside combustion chamber as it can be seen that the swirl is already generated at some location of cylinder wall during intake stroke. As indicated by the symmetrical projections of the streamlines, the flows are seen to be quite symmetrical about the centre plane between two valves due to the symmetrical runner, port and valve setting. This symmetrical flow structure and pattern implies that the bulk flows from the two valve openings do not mix together significantly. As can be seen, the blue line of piston A streams cylindrically inside cylinder when the air comes in from intake port at the maximum valve lift if comparing to the air mixture of piston B. This condition will give a clear phenomenon that the piston A can be adopted to give a homogeneous condition, which provided by the CFD calculation instead of experimental test. It is also interesting to notice in the computation that the detailed investigation of air motion (swirls and tumbles behaviour) in the combustion chamber can be carried out by using the CFD code.

## NUMERICAL VALIDATION

A numerical validation was provided as a proof that the performed CFD simulation has been correct and accurate with the experimental study. The validation is presented in the form of in-cylinder pressure during intake and compression stroke between the CFD code and available experimental data. In this section, the comparison between simulated and experimental in-cylinder pressure under motoring condition is presented according to a certain engine operating conditions and speed.

The experimental setup for the purpose of validating the CFD simulation was carried out in a test rig of Single Cylinder Research Engine (SCRE) as shown in Fig. 17. The available data used for the numerical validation was performed by considering some important technical aspects. During the experiment, all engine boundary conditions were fixed. Piezoelectric pressure sensors (Kistler 6061B) were installed on the combustion chamber to measure the cylinder pressure occurred during combustion process. In order to obtain the boundary conditions at intake and outflow boundaries for the CFD analysis, thermocouple sensor were installed at nearest possible to the cylinder head so that the temperature of intake and exhaust ports can be determined to be used inside CFD simulation. The fuel injection supply and ignition timing was controlled intelligently by an Electronic Control Unit (ECU) installed inside the engine. The shape of piston crown used for the present validation study is the piston A due to the reason that the piston A had been inserted inside the test rig initially, while piston B has not available yet for the experimental study.

The comparison was performed in the engine speed of 2000 rpm. The measurement data for intake port temperature and pressure are 302 K and 1.02 bar, respectively. These two data was applied into

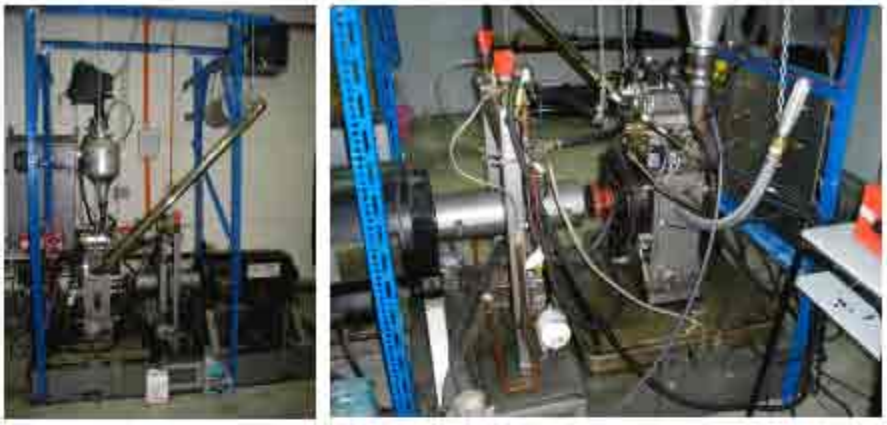

Fig. 17: The SCRE test rig of CNG-DI engine

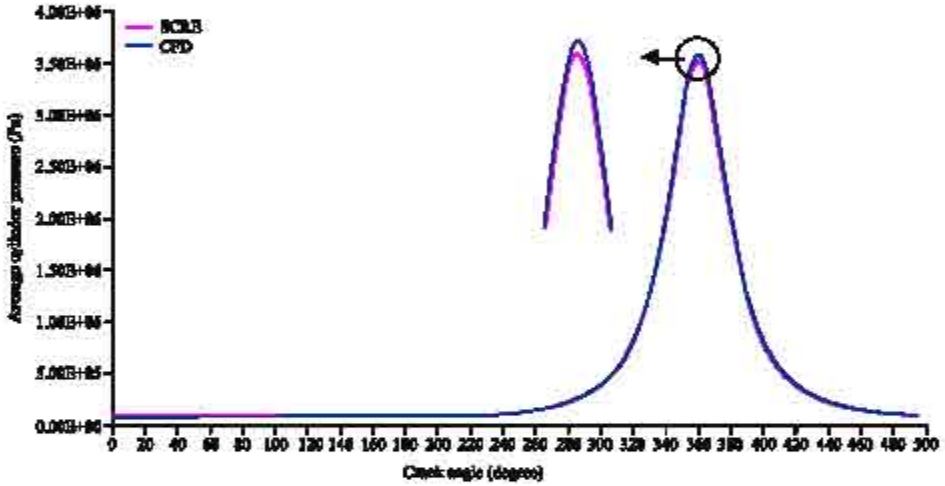


Fig. 18: Calculated and measured in-cylinder pressure under motoring condition

computational mesh for CFD analysis to represent the real engine modelling. Figure 18 illustrates a comparison between the calculated and experimental pressure curves under the motoring condition during intake and compression stroke. It is indicated that the calculated maximum pressure is in a close agreement with the measured result. Therefore, the CFD computational mesh and calculation performed in this investigation of turbulence characteristics are able to represent the real condition occurred inside the CNG-DI engine and have the capability to be implemented for further intensive calculation. As can be seen, the cylinder pressure obtained from the CFD simulation has the higher value due to the reason that the typical CFD simulations do not take into account the friction losses took place within engine cylinder. Hence, the numerical calculation has the higher cylinder pressure compared to the experimental data and it is usually accepted for any validation of simulation results.

The actual validation of the numerical prediction from CFD results in an internal combustion engine is through the utilisation of some high-cost visualisation equipment, such as Particle Image Velocimetry (PIV), Laser Doppler Anemometry (LDA) or any visualisation method. In this study, the limitation of high investment on those equipments has become an obstacle to employ it to validate the CFD data. Therefore, besides the in-cylinder pressure comparison during motoring condition, the other technique of numerical assessment used to validate the results obtained from CFD calculation in this research is the typical swirl and tumble ratio produced from the other researchers.

Theoretically, the magnitude of fluid flow and turbulence parameters are depend on the engine size, speed, valve opening and closing timing, bore and stroke, piston crown, initial pressure and temperature and other engine configuration. For swirl and tumble ratio, the magnitude obtained in this study are in the range of typical value of swirl and tumble ratio based on the current literature review (Kim *et al*., 1999; Heywood, 1987; Suh and Rutland, 1999; Han and Reitz, 1997; Luo *et al*., 2003; Bailly *et al*., 1999; Han *et al*., 1997; Han and Reitz, 1995). Therefore, the investigation on the effect of piston crown to the dynamic flow and turbulence in this study, which results some parameters mentioned above have adequate comparison to be recognised as a valid and accurate CFD result.

## CONCLUSIONS

The investigation and analysis for the characteristics of in-cylinder air motion under motoring condition is numerically carried out by solving intake and compression stroke by CFD code with the moving mesh and boundary capability. Transient moving valves were exactly modelled to resolve intake-generated swirl and tumble motion characteristics in the area of valve curtain and engine cylinder. The evaluation in present study is carried out for two shapes of piston crown to evaluate the effect of different combustion chamber shape to the fluid flow field for the preparation of air-fuel mixture before fuel injection begins. The solved calculation of CFD analysis for every crank angle throughout intake and compression stroke is presented to examine and verify the behaviour of those mentioned characteristics for overall piston crowns furnished with its discussions thoroughly.

The global variations of each characteristic versus crank angle during intake and compression stroke has been determined to exhibit the effect of combustion chamber shape within engine cylinder. During intake stroke the shape of the piston crown does play a significant role to the developed large scale fluid motion as the most significant component of mixing parameters during the whole process of engine by characterising it with the swirl ratio, sideways and normal tumble ratio.

In general, this study shows that in-cylinder CFD predictions yield a reasonable result that allows improving the knowledge of the in-cylinder flow pattern and characteristics during intake and compression strokes instead of using the experimental test by Particle Image Velocimetry (PIV) or laser Doppler anemometry (LDA). At this moment, this CFD in-cylinder analysis result has not been validated with the experimental result of flow visualisation due to the highly experimental equipments, devices and measurement tools. However, the cylinder pressure of motoring condition has been validated against the experimental measurement and it reveals that the developed engine model and its moving mesh have a capability to approach the real engine condition. In addition, the study and analysis presented here represents a first step towards our understanding of air motion field inside cylinder for an automotive four-stroke internal combustion engine with fuel direct injection system. Besides of that, CFD can be used as an efficient design tool to develop the other internal combustion engine analysis to produce an optimum engine configuration. For future work, the application of Large Eddy Simulation (LES) model to investigate the behaviour of fluid flow in an internal combustion engine can be performed for better understanding of these complex phenomena of fluid dynamic, such as the work has been done by Haworth (2000), Lee and Lee (2006) and Thobois *et al*. (2005). However, the relatively high computation cost will be occurred as a consequence from the use of LES model due to their numerical algorithm and the hardware resources to carry out this kind of huge task is not adequate for us to perform at the moment. Lastly, the optimum piston crown investigated from the present study, which is piston A will be used as a further examination by carrying out it into the combustion and emission formation analysis.

## ACKNOWLEDGMENTS

The authors would like to thank the Ministry of Science, Technology and Innovation of Malaysia for sponsoring this work under project IRPA 03-02-02-0057-PR0030/10-04.

## REFERENCES

Bailly, O., C. Buchou, A. Floch and L. Sainsaulieu, 1999. Simulation of the intake and compression strokes of a motored 4-valve SI engine with a finite element code. Oil and Gas Science and Technology-Rev. IFP, 54: 161-168.

CD Adapco, 2004. STAR-CD Version 3.22 User Manual and Methodology. Adapco Group Press.

Celik, I., I. Yavuz and A. Smirnov, 2001. Large eddy simulations of in-cylinder turbulence for internal combustion engines: A review. Int. J. Eng. Res., 2: 119-48.

Chen, A., A. Veshagh and S. Wallace, 1998. Intake flow predictions of a transparent DI Diesel engine. SAE Paper, 981020.

Dillies, B., A. Ducamin, L. Lebrere and F. Neveu, 1997. Direct injection Diesel engine simulation: A combined numerical and experimental approach from aerodynamics to combustion. SAE Paper, 970880.

Gosman, A.D., Y.Y. Tsui and A.P. Watkins, 1984. Calculation of Three Dimensional Air Motion Model Engines. SAE Paper, 840229.

Han, Z. and R.D. Reitz, 1995. Turbulence modeling of internal combustion engines using RNG k-ε models. Combustion Sci. Technol., 106: 267-295.

Han, Z.Y. and R.D. Reitz, 1997. Multidimensional modeling of spray atomization and air-fuel mixing in a direct-injection spark-ignition engine. SAE Paper, 970884.

Han, Z.H., R.D. Reitz, J.L. Yang and R.W. Anderson, 1997. Effects of injection timing on air-fuel mixing in a direct-injection spark-ignition engine. SAE Paper, 970625.

Haworth, D.C., 2000. Large-eddy simulation on unstructured deforming meshes: Towards reciprocating IC engines. Comput. Fluids, 29: 493-524.

Heywood, J.B., 1987. Fluid motion within the cylinder of internal combustion engine. The 1986 Freeman Scholar Lecture. J. Fluids Eng., 109: 3-35.

Heywood, J.B., 1988. Internal Combustion Engine Fundamentals. McGraw-Hill Inc., New York.

Hyun, G., M. Oguma and S. Goto, 2002. 3-D CFD analysis of the mixture formation processes in an LPG DI SI engine for heavy duty vehicles. In Proceedings of the 12th Int. Conf. Multidimensional Engine Modelling User Group Meeting SAE Congress, 3-5 March, Detroit, Michigan, United States of America.

Kim, Y.J., H.L. Sang and H.C. Nam, 1999. Effect of air motion on fuel spray characteristics in a gasoline direct injection engine. SAE Paper, 1999-01-0177.

Launder, B.E. and D.B. Spalding, 1974. The numerical computation of turbulent flow. Comput. Methods Applied Mechanics Eng., 3: 269-289.

Lee, B.S. and J.S. Lee, 2006. Large eddy simulations of tumble and swirl formations in engine in-cylinder flow. Int. J. Automotive Technol., 7: 415-422.

Luo, M.J., G.H. Chen and Y.H. Ma, 2003. Three-dimensional transient numerical simulation for intake process in the engine intake port-valve-cylinder system. J. Zhejiang Univ. Sci., 4: 309-316.

Mao, Y., M. Buffat and D. Jeandel, 1994. Simulation of the turbulent flow inside the combustion chamber of a reciprocating engine with a finite element method. J. Fluid Eng., 116: 363-369.

Payri, F., J. Benajes, X. Margot and A. Gil, 2004. CFD modelling of the in-cylinder flow in direct-injection Diesel engines. Comput. Fluids, 33: 995-1021.

Stone, R., 1992. Introduction to Internal Combustion Engines. The Macmillan Press Ltd., London.

Suh, E.S. and C.J. Rutland, 1999. Numerical study of fuel/air mixture preparation in a GDI engine. SAE Paper, 1999-01-3657.

Sukegawa, Y., T. Nogi and Y. Kihara, 2003. In cylinder airflow of automotive engine by quasi-direct numerical simulation. JSAE Rev., 24: 123-126.

Thobois, L., G. Rymer, T. Souleres, T. Poinsot and B. Van Den Heuvel, 2005. Large Eddy Simulation for the prediction of aerodynamics in IC engines. Int. J. Vehicle Design, 39: 368-382.

Versteeg, H.K. and W. Malalasekera, 1995. An Introduction to Computational Fluid Dynamics-The Finite Volume Method, Longman Group Ltd. London.

Wu, H.W. and S.W. Perng, 2004. Numerical analysis of thermal turbulent flow in the bowl in piston combustion chamber of a motored engine. Int. J. Therm. Sci., 43: 1011-1023.